Supplementary Information for

Central Role of Autophagic UVRAG in Melanogenesis and the Suntan Response

Yongfei Yang[a,1], Gyu-beom Jang[a,1], Xuanjun Yang[b,c], Qiaoxiu Wang[a], Shanshan He[a], Shun Li[a,d], Christine Quach[a], Shihui Zhao[a], Fan Li[e], Zengqiang Yuan[f], Hye-Ra Lee[g], Hanbing Zhong[c], and Chengyu Liang[a,2]

[a]Department of Molecular Microbiology and Immunology, Keck School of Medicine of the University of Southern California, Los Angeles, CA 90033;
[b]Institute of Chinese Medical Sciences, University of Macau, Macao, China;
[c]Department of Biology, South University of Science and Technology, 518055 Shenzhen, China;
[d]Key Laboratory of Biorheological Science and Technology, Ministry of Education, College of Bioengineering, Chongqing University, 400044 Chongqing, China;
[e]Division of Infectious Diseases, Department of Pediatrics, Children's Hospital Los Angeles, Los Angeles, CA 90027;
[f]Brain Science Center at the Institute of Basic Medical Sciences, Haidian District, 100850 Beijing, China
[g]Department of Biotechnology and Bioinformatics, Collage of Science and Technology, Korea University, 30019 Sejong, Republic of Korea

[1] Y.Y. and G.-b.J. contributed equally to this work.
[2] To whom correspondence should be addressed.

Lead Contact information:

Chengyu Liang
E-mail: chengyu.liang@med.usc.edu

This PDF file includes:

Supplementary text

Figs. S1 to S8

Tables S1 to S2

References for SI reference citations

Supplementary Information Text

Materials and Methods

Cell Culture and Transfection. HEK293T, B16, A375, G361, SK-MEL-5 and MeWo cells were cultured in Dulbecco's modified Eagle's medium (DMEM) supplemented with 10% fetal bovine serum (FBS; Invitrogen), 2 mM L-glutamine and 1% penicillin-streptomycin (Gibco-BRL). Primary human melanocytes (ATCC, PCS-200-013) were cultured in medium 254 (Thermo, M254500) supplemented with human melanocyte growth supplement (Thermo, S0025) and 1% penicillin-streptomycin. Human melanocytes were immortalized by the HPV E6/E7. We employed a retroviral construct to introduce HPV E6/E7 into human primary melanocytes. Transfected cells were selected by neomycin resistance and continuously cultured for expansion. Mouse melanocytes (ATCC, CRL-2770) were cultured in Ham's F10 medium supplemented with 50 ng/ml TPA (SigmaAldrich # P-8139) and 7% horse serum. Human keratinocytes (Lifeline cell tech, FC-0025) were maintained in DermaLife K keratinocyte Medium Complete Kit (Lifeline cell tech, LL-0007). Transfections were performed with Calcium Phosphate Transfection Kits (Clontech) or Lipofectamine 2000 (Invitrogen), following the manufacturer's instructions.

Generating UVRAG Knockout Cell by CRISPR-Cas9 Nickase. *UVRAG* sgRNAs were designed using the CRISPRtool (http://crispr.mit.edu) to minimize potential off-target effects. sgRNA sequences and genomic primers are listed in Table S2. Two pair of oligos were annealed, phosphorylated, and ligated to the *Bsa* I site of pGL3-U6-sgRNA-PGK-Puro vector (Addgene, 51133). Two mouse UVRAG sgRNA plasmids and Cas9 nicknase expression plasmid (pST1374-Cas9-N-NLS-flag-linker-D10A; Addgene 51130) were transfected into B16 cells with a ratio of 1:1:2 using PolyFect transfection reagent (Qiagen 301105). After 24 hrs, the transfected cells were selected in 1 μg/ml puromycin and 10 μg/ml Blasticidin for 2 days. After 72 hrs transfection, cells were split into 96-wells plates to form single cell clones. After 7 to 10 days, individual colonies were picked and genomic DNA was extracted using Quick Extract DNA extraction solution (Epicentre; USA) following the recommended protocol.

Genomic DNA of each single clone was PCR amplified using high-fidelity polymerases and sequenced to confirm the UVRAG deletion mutant. The homozygous deletion of UVRAG was further confirmed by Western Blotting.

Plasmids. The full-length cDNA clones of MITF-M (plasmid# 31151), BRAF (V600E) (plasmid # 15269), and human UVRAG (plasmid# 24292) were purchased from Addgene (USA). The Flag-, GFP- or HA-tagged WT MITF, UVRAG, and their mutant derivatives were constructed by cloning the cDNA of the full-length or truncated mutants into the pcDNA5/FRT/TO vector. Flag-MITF and UVRAG constructs were also cloned into pCDH-CMV-MCS-EF1-Puro backbone to generate lentiviral transfer constructs. The cDNA of OA1 is a gift from Dr. Elena Oancea. GFP- and mCherry-tagged OA1 was cloned into pCDH-CMV-MCS-EF1-puro backbone to generate lentiviral transfer constructs. The Flag- and GFP-tagged BRAF(V600E) was cloned into pCDH-CMV-MCS-EF1-Puro backbone to generate lentiviral transfer constructs. All constructs were confirmed by sequencing using an ABI PRISM 377 automatic DNA sequencer (Applied Biosystems, Foster City, CA).

Antibodies and Other Reagents. The following antibodies were used in this study: UVRAG (U7058, Sigma-Aldrich); UVRAG (SAB4200005, Sigma-Aldrich); UVRAG (SC-82115, Santa Cruz); p-UVRAG (Ser 498) (ABS1600, Millipore); p62 (5114S, Cell Signaling); LC3B (2775S, Cell Signaling); Beclin1 (612113, BD Bioscience); Atg5 (A0731, Sigma-Aldrich); Atg16 (ab47946, Abcam); MITF-M (MA5-14146, Clone C5, Thermo); MITF-M (ab12039, ChIP Grade, Abcam); MITF-M (ab140606, Abcam); TYR (ab738, Abcam); TYR (sc-7833, Santa Cruz); TYRP1 (SAB2102617, Sigma-Aldrich); TYRP1 (NBP2-32906, Novus); DCT (SAB4500626, Sigma-Aldrich); PMEL (ab137078, Abcam); PMEL (NBP2-29418, Clone HMB45, Novus); TFEB (PA5-34360, Thermo); BLOS1 (PA5-41425, Thermo); BLOS2 (PA5-25452, Thermo); BLOS3 (ab130997, Abcam); Snapin (148002, Synaptic Systems), Pallidin (10891-2-AP, Proteintech); Myrlysin (17169-1-AP, Proteintech); Cappucino (NBP1-91798, Novus); Muted (24015-1-AP, Proteintech); Dysbindin (11132-1-AP, Proteintech); TFE3 (ab179804, Abcam); Actin (sc-47778, Santa Cruz); Flag (F3165, Sigma-Aldrich); Flag (F2555, Sigma-Aldrich); HA

(NB600-363, Novus), HA (H6533, Sigma); HRP-labeled or fluorescently labeled secondary antibody conjugates, purchased from Molecular Probes (Invitrogen). α-MSH (ab120189), IBMX (ab120840), Forskolin (ab120058), and PLX4720 (ab141362) were obtained from Abcam. The working concentration of α-MSH, forskolin and IBMX, and PLX4720 used in the study is 2 μM, 10 μM, and 1 μM, respectively.

Immunoprecipitation and Immunoblotting. For immunoprecipitation, cells were washed with ice-cold PBS, lysed in 2% Triton X-100 lysis buffer (20 mM Tris at pH 7.5, 150 mM NaCl, 1 mM EDTA and 2% Triton X-100), supplemented with a phosphatase inhibitor mix (Pierce) and a complete protease inhibitor cocktail (Roche). After sonication (amplitude 15%, process time 10s, push-on time 5s, and push-off time 1s), cell lysates were rotated at 4°C for at least 30 min, and then the soluble fraction was isolated by centrifugation at 14,000 rpm for 10 min at 4 °C, which was subjected to pre-clearing with protein A/G agarose beads for 1 h at 4 °C, whole-cell lysates (WCL) were used for immunoprecipitation (IP) with the indicated antibodies. Generally, 1-4 μg commercial antibody was added to 1 ml WCL, which was incubated at 4°C for 8-12 hr. After addition of protein A/G agarose beads, incubation was continued for another 2 hr. Immunoprecipitates were extensively washed with IP wash buffer 10 mM Tris at pH 7.5, 150 mM NaCl, 1 mM EDTA, 0.2% Triton X-100, 1x phosphatase inhibitor mix (Pierce), and 1x protease inhibitor mix (Roche), and eluted with SDS–PAGE loading buffer by boiling for 5 min. For immunoblotting, polypeptides were resolved by SDS–PAGE and transferred to a PVDF membrane (BioRad). Membranes were blocked with 5% non-fat milk, and probed with the indicated antibodies. Horseradish peroxidase (HRP)-conjugated goat secondary antibodies were used (1:105,000, Invitrogen). Immunodetection was achieved with the Hyglo chemiluminescence reagent (Denville Scientific), and detected by a Fuji ECL machine (LAS-3000).

Protein Purification. The full-length cDNA fragments of MITF, UVRAG, and BLOS1 were cloned into the pGEX-4T-1 vector (for MITF and UVRAG) and to the pRSET-C vector (for BLOS1). The resulting plasmid was used to transform the BL21(DE3) bacteria strain and the GST-UVRAG, GST-MITF, and

His-BLOS1 proteins were induced by 0.5 mM isopropyl β-D-1-thiogalactopyranoside (IPTG). Cells were collected by centrifuge and cell pellets were freeze-thawed for three times, then re-suspended in pre-chilled PBS buffer with protease inhibitors (Thermo Fisher), followed by sonication for 15 s at amplitude 15%. Cell debris was spun-down and the clarified supernatant was loaded onto a Glutathione–Agarose (Sigma G4510) column (for GST-MITF and GST-UVRAG) or a Ni-NTA (Qiagen 30622) column (for His-BLOS1) under gravity flow. After three-time ice-cold PBST (PBS containing 1% Triton X-100) wash, proteins were eluted with the elution Buffer (50 mM reduced glutathione in PBS, 1 mM DTT, pH 9.0) at room temperature for approximately 30 min. The eluted proteins were analyzed by electrophoresis on 4-20% Tris-Glycine gels followed by Coomassie blue staining.

Immunofluorescence, Confocal Laser Scanning Microscopy. Immunofluorescence microscopy was carried out as described previously(1). Briefly, cells plated on coverslips were fixed with 4% paraformaldehyde (20 min at RT). After fixation, cells were permeabilized with 0.1% Triton X-100 for 10 min and blocked with 10% goat serum (Gibco) for 1 hr. Primary antibody staining was carried out using antiserum or purified antibody in 1% goat serum for 1-2 hr at room temperature or overnight at 4 °C. Cells were then extensively washed with phosphate-buffered saline (PBS) and incubated with Alexa 488-, Alexa 568-, and/or Alexa 633-conjugated secondary antibodies in 1% goat serum for 1 h, followed by DAPI (4', 6'-diamidino-2-phenylindole) staining. Cells were mounted using Vectashield (Vector Laboratories, Inc.). Confocal images were acquired using a Nikon Eclipse C1 laser-scanning microscope (Nikon, PA) fitted with a 60x Nikon objective (PL APO, 1.4NA).

For image quantification in Figure 1J and 2C, approximately 200 cells, randomly chosen from 10 high power field and pooled from three independent experiments, were evaluated for the distribution pattern of the indicated molecules. The Pearson correlation coefficient in Figure 2D was calculated using the built-in colocalization analysis module of the NIS-Elements AR software. All experiments were independently repeated several times. The investigators conducted blind counting for each quantification-related study.

Melanin Determination Assay. Measurement of melanin content was performed as previously described(2-4). Briefly, equal numbers of melanocytes were collected, washed twice with PBS, and resuspended in 1N NaOH (in 20% DMSO) for 45min at 95°C. The mixed homogenate were centrifuged for 10 min at 1000g, and the resulting supernatant (100 μl) was placed in a 96-well microplate and optical densities (ODs) were measured at 405 nm. The protein concentration of each cell sample was determined using the Bradford assay (Bio-Rad, Hercules, CA, USA). Relative melanin production was calculated by normalizing the OD values with the protein concentrations (absorbance/ μg protein).

Conventional Electron Microscopy. Conventional electron microscopy was performed as previously described(4). Briefly, B16 cells were fixed overnight at 4˚C in 1/2 strength Karnovsky's (2% paraformaldehyde and 2.5% glutaraldehyde in 0.2 M sodium cacodylate buffer, pH 7.4). Cells were rinsed in 0.1 M sodium cacodylate buffer and pelleted. Cell pellets were treated with 2% osmium tetroxide in 0.2 M cacodylate buffer for 2 hr at 4˚C, and rinsed in 0.1 M cacodylate buffer. Small pieces were dehydrated through a graded series of ethanol, and then infiltrated with Epon resin overnight at room temp. They were then embedded in resin overnight at 60°C. Thin sections were cut on a Leica UC6 ultramicrotome, collected onto formvar-carbon coated slot grids. Before visualization, samples were stained in 1% aqueous with uranyl acetate for 2 hours and lead citrate for 5 min, and examined with a JEOL 2100 transmission electron microscope.

Flow Cytometry Analysis. All flow cytometry experiments were performed in triplicate and repeated at least three times, using 10,000 ~ 20,000 cells per replicate. Melanocytes constitutively expressing OA1-GFP or OA1-mCherry were cultured with log-phase growth. The cells were then harvested with cell dissociation buffer (Sigma Aldrich), rinsed with PBS containing 0.05% saponin to remove soluble contents, and washed twice with PBS. Green or red melanosome fluorescence of cells per sample was determined by flow cytometry using the BD FACSAria cytometer (BD Biosciences).

Gene Knockdown by shRNA and Lentiviral Gene Delivery. All shRNA plasmids were purchased from Open Biosystem. Lentiviral shRNA sequence targeting UVRAG is: 5'-ACGGAACATTGTTAATAGAA-3'; targeting MITF are: 5'-GGTGTAGTATTAATAGGTTAA-3' and 5'-CCTTTCTACCACTTTAGCAAATA-3'; targeting TFE3 are: 5'-GCCTGGAGTCCAGTTACAATG-3'; 5'-GGACAGATTATGAAATTTCAT-3'); targeting TFEB are: 5'-GCCTGGAGTCCAGTTACAATG-3' and 5'-GGACAGATTATGAAATTTCAT-3'; targeting BLOS1 is: 5'-GCACTGGAATATGTCTACAAA-3'; targeting Pallidin is: 5'-CCAGTAACTCTTGGGATTAAT-3'; targeting Beclin1 is: 5'-GCCAATAAGATGGGTCTGAAA-3'; targeting Atg5 is: 5'-CTTGGAACATCACAGTACA-3'; targeting Atg16 is: 5'-CCAACAGAACTTGATTGTAAA-3'

For lentivirus production, HEK293T cells were transfected with the transfer vector (e.g. pCDH-CMV-MCS-EF1-Puro or pGIPZ), pCMV-dR8.91 packaging plasmid, and pCMV-VSV-G envelope plasmid in a 6:5:1 ratio using Calcium Phosphate Transfection Kits (Clontech). The medium was refreshed 12 hrs later. Viral particles were collected 48 hrs after transfection, filtered with 0.45 μm sterile filter, and concentrated by ultracentrifugation at 4°C (24000 rpm, 2 hr, Beckman-Coulter ultracentrifuge XL-100K). Viral particles were resuspended in fresh medium with 8 μm/ml polybrene, and were placed on target cells for 24 hrs. Lentivirally-transduced cells were selected in 2 μg/ml puromycin for 2 days.

Yeast Two-hybrid. To identify UVRAG-interacting proteins, yeast two-hybrid was performed using Matchmaker Two-hybrid system 3 (Clontech), according to the previously published method(5). Yeast strain AH109, which contains the Gal4-UVRAG full-length fusion gene plasmid, was grown overnight in synthetic dropout (SD)/-Trp medium to a density of approximately 10^7 cells/ml, diluted in 1 liter of warmed -Trp medium to an optical density (OD 600) of 0.2~0.3, and grown to an exponential stage. The cells were harvested and washed twice with 100 ml of water and once with TE (Clontech, CA). The pellet was resuspended in 8 ml of 10 mM Tris-HCl (pH 7.5), 1 mM EDTA, and 0.1 M Li-acetate (LiOAc). The suspension was then mixed with 1 mg of transforming DNA and 20 mg of single-stranded salmon sperm DNA, after which 60 ml of a solution consisting of 40% polyethyleneglycol-

3350 in Tris-EDTA-LiOAc was added and thoroughly mixed, followed by incubation with agitation at 30°C for 30 min. After a heat pulse at 42°C for 15 min, the cells were pelleted, resuspended with YPD, and plated on selective medium. Library screening and recovery of plasmids were performed according to the manufacturer's instructions.

Electrophoretic Mobility Shift Assay (EMSA). Binding activity of purified MITF to the DNA probes (listed in Supplementary information, Table S2) was measured by a gel mobility shift assay (6) with modification. The E-box WT and mutant fragments of UVRAG were generated using the directed mutagenesis kit (NEB E0554) and verified by sequencing. All of the DNA probes were purified using QIAquick PCR purification kit (Qiagen 28104). The EMSA essay was performed using Thermo E33075 kit following the instruction. Briefly, 100 ng DNA probes and 300 ng purified recombinant MITF proteins were mixed thoroughly and incubated in the binding buffer for 40 minutes at room temperature. At the end of the incubation, 6X EMSA gel-loading solution was added and the DNA–protein complexes were separated by electrophoresis using a non-denaturing polyacrylamide gel. The gel was then washed with ddH2O and incubated in the 1X SYBR Green staining solutions for 20 minutes and protected from light. Excess stain of the gel was washed again in ddH_2O for 10 seconds for three times. The stained DNA probes were visualized using the Gel Doc system (Bio-Rad).

Chromatin Immunoprecipitation (ChIP) Analysis. ChIP was performed as described previously(7) using MAGnify™ Chromatin Immunoprecipitation System (Thermo 492024) according to the manufacture instruction. Briefly, melanocytes were crosslinked with 1 % formaldehyde for 10 min at room temperature and quenched with 0.125 M glycine. Cells were lysed in lysis buffer (25 mM Tris–HCl, pH 7.5, 150 mM NaCl, 1% Triton X-100, 0.1% SDS, 0.5% deoxycholate, with proteinase inhibitors and micrococcal nuclease). The lysates were sonicated for 10 x 20 s (30% output) using MISONIX sonic processors, cleared by centrifugation for 10 min at 4°C, and diluted in 9 volumes of dilution buffer (1% Triton X-100, 2 mM EDTA, 150 mM NaCl, 20 mM Tris-HCl pH 7.5). Diluted chromatines were incubated with appropriate antibody-Dynabeads protein A/G complexes for binding

overnight at 4˚C for immunoprecipitation. Beads were washed twice with RIPA buffer, once in high salt buffer (50 mM Tris–Cl, pH 8.0, 500 mM NaCl, 0.1% SDS, 0.5% deoxycholate, 1% NP-40, 1 mM EDTA), once in LiCl buffer (50 mM Tris–Cl, pH 8.0, 250 mM LiCl, 1%NP-40, 0.5% deoxycholate, 1 mM EDTA) and twice in TE buffer (10 mM Tris–Cl, pH 8.0, 1 mM EDTA, pH 8.0). Beads were resuspended in TE containing 50 mg/ml of RNase and incubated for 30 min, then washed with water and eluted with elution buffer (1% SDS, 0.1 M NaHCO3) for 15 min. Crosslinks were reversed by adding 200 mM NaCl followed by an incubation for 6 hr at 65°C. Samples were deproteinized overnight with proteinase K and DNA was extracted with phenol–chloroform followed by ethanol precipitation. DNA associated with immunoprecipitated proteins was then quantified by real-time PCR with the primer set adjacent to the gene promoters as listed in Table S2. All experimental values were normalized to the input DNA using amplification of GAPDH.

Luciferase Reporter Assays. The human UVRAG promoter was amplified by PCR from the genomic DNA of 293T cells, and cloned into the pGL-4.23 vector. The mutant reporter plasmids were generated using the directed mutagenesis kit (NEB E0554) and verified by sequencing. The melanocyte and 293T cells were transfected with the promoter construct along with the pRL-CMV Renilla luciferase reporter plasmid as an internal control using polyfect transfection reagent (Qiagen 301107). Cells were lysed 48 hr after transfection and assayed with the dual-luciferase reporter assay system (Promega E1910), and measurements made on the Beckman-Coulter DTX880. At least four replicates with three independent experiments were performed, transfection efficiency were normalized using Renilla luciferase.

Tyrosinase Activities. Tyrosinase activity was measured as previously described(8). Briefly, cells were washed in ice-cold PBS, lysed in Triton X-100 lysis buffer (20 mM Tris-Hcl pH 7.5; 150 mM NaCl; 1 mM EDTA; 2% Triton X-100), and centrifuged at 13,000g for 20 minutes at 4 ˚C. L-DOPA in PBS (final conc. 0.3 mg/mL) was then added to supernatants and lysates were incubated at 37 ˚C for 2 hrs.

OD405 was measured upon color change by Beckman-Coulter DTX880. Data was normalized to protein concentration by Bradford (Bio-Rad).

RNA extraction, cDNA synthesis, and Real-time PCR Analysis. Total RNA was isolated with RNeasy Mini Kit (Qiagen 74104), and 1 μg of total RNA was used for cDNA synthesis using iScript™ cDNA Synthesis Kit (Bio-rad). Quantitative real-time PCRs were carried out using the primers listed in Table S2 and the iQ SYBR Green Master Mix (Bio-rad). Samples were obtained and analyzed on the CFX96 Touch Real-Time PCR Detection System. The gene expression levels were normalized to Actin.

Zebrafish Maintenance and Imaging. Wild type TU zebrafish were raised and bred under standard conditions in the South University of Science and Technology of China Zebrafish Facility. All experiments were approved by the Institute Animal Ethics Committee. Embryos were staged by hours or days post fertilization at 28.5˚C (hpf or dph) as described previously(9). Zebrafish embryos at 10 or 30 dpf were collected and fixed in 4% paraformaldehyde in PBS at room temperature for 3-5 hours. The embryos were mounted in 2.5% methyl cellulose and images were taken with BX53 microscope and DP73 digital camera (Olympus, Japan), and edited with Photoshop CS 6.0. 50 fish from each condition were pooled for imaging analysis.

Morpholino Oligonucleotide (MO) Design and Injection and EGFP Reporter Assay. Antisense MO against the ATG translation initiation site of target genes were designed and synthesized from Gene Tools (Philomath, OR): *uvrag* MO, 5'-ATGAACTCCATCGCCGGTCGGGATC-3', *tyr* MO, 5'-TGTGTGTGAAGCGTCTCACTCTCCT-3', *pmel* MO, 5'-TCATCATGTGGACATCTCTCATCTT-3'. The MO target sites was then sub-cloned into the *Hind* III and *BamH* I sites of pCS2+EGFP vector. The target sites were introduced to the 5' end of EGFP to assure the downstream EGFP is in frame. Target insertion in the vectors was confirmed by sequencing. MO were dissolved in nuclease-free water and stored in -20°C. Before injection, MOs were denatured at 65°C for 5 min and quickly spun

to avoid the formation of aggregates and 5 μl were loaded in a microinjection machine. Embryos at one or two cell stages were injected with 2.5 ng of antisense targeting-MO or standard control oligo and allowed to grow to the larval stage. Following morpholino injections, embryos were excluded at 1 dpf. For the quantification of pigmentation, the magic wand tool of Photoshop (tolerance is 20) is used to select the pigmented region above ear as indicated by the red square. Photoshop automatically shows the number of pixels and mean gray value of selected region. We use pixels*255/mean gray value to calculate the pigmentation and normalize it to control MO group. Quantitative statistical data are shown as the mean ± standard error of the mean (SEM) of each group. *p*-values of group comparisons were obtained by using unpaired two-tailed Student's *t*-test analysis. Statistical significance was concluded when P-values were < 0.05.

RNA Rescue Experiment. Full-length *uvrag* excluding the 5' UTR sequence containing the morpholino target site was cloned into the pcDNA3.1 vector. To make 5'-capped RNA, plasmids was linearized with Dra III and subjected to in vitro transcription with T7 RNA polymerase in the presence of 0.5 mM Ribo m7G Cap Analog (Promega). RNA was purified by RNeasy mini kit (Qiagen) according ot the manufacturer's instructions. uvrag 5'UTR antisense MO was injected at 0.2 mM with or without 70 ng/ul capped uvrag RNA. uvrag RNA was injected alone as a control for RNA toxicity.

ChIP-seq and Gene Expression Analysis of Publically Available Datasets. The MOTF and YY1 ChIP-seq data were obtained from two published papers (10, 11). All gene expression data of melanoma were retrieved from TCGA (https://tcga-data.nci.nih.gov/tcga), and cBioPortal (http://www.cbioportal.org/public-portal/)(12, 13). All statistical analyses were carried out using the R software package and GraphPad Prism 6.0 (GraphPad Software, Inc.).

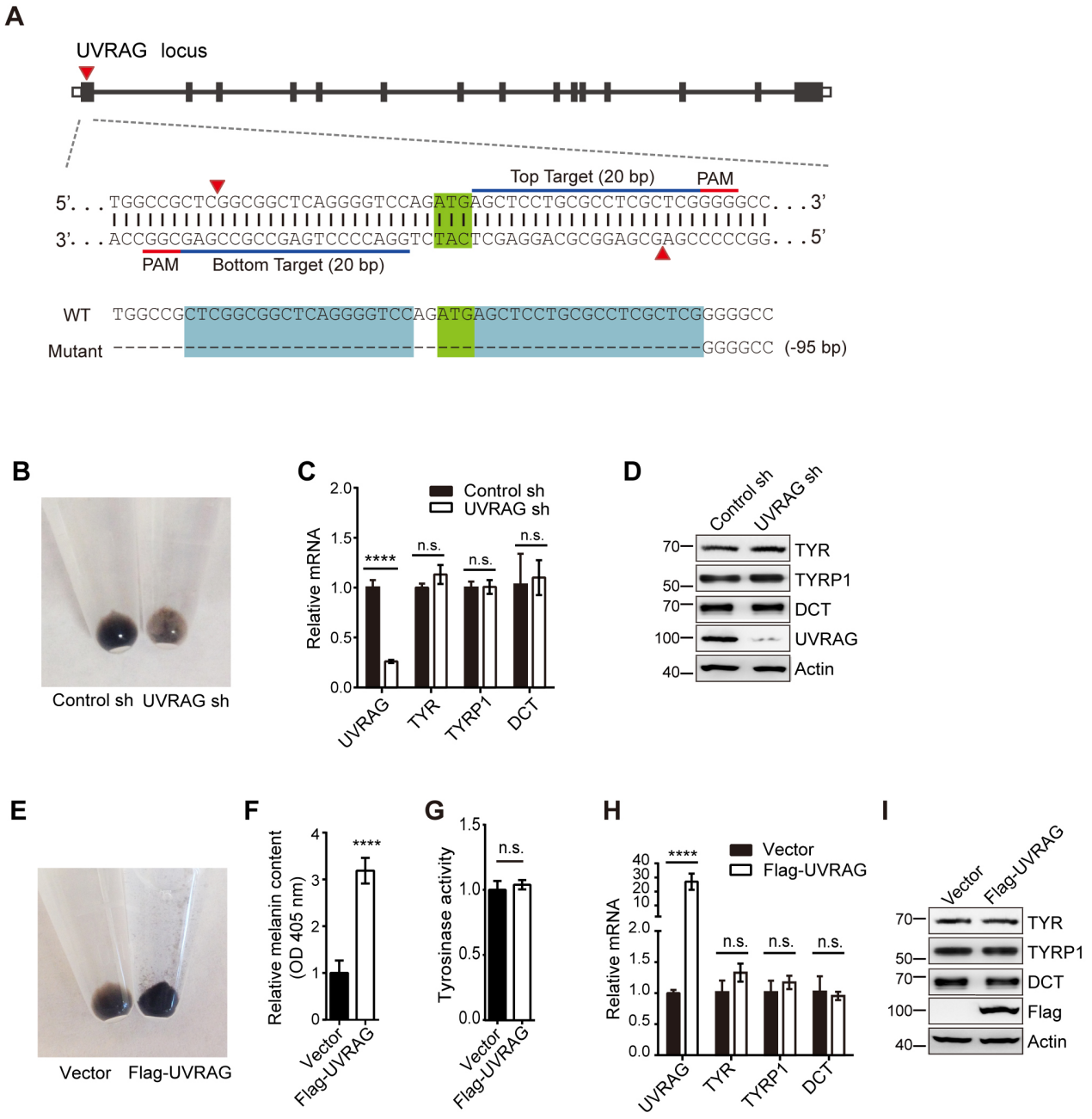

Fig. S1. Related to Fig. 1: The role of UVRAG in cell pigmentation. (*A*) Single-guide RNA (sgRNA) design for targeting the mouse *UVRAG* locus (top) and sequence of targeted locus (bottom) in single-cell clones of B16 cells. (*B*) Cell pellets of B16 cells expressing control shRNA or shRNA against UVRAG after 6-day culture are shown. (*C*) Relative mRNA expression of the indicated gene in cells in (*B*). Data shown represent mean ± SD from three independent experiments. ****, $p < 0.0001$; n.s., not significant. (*D*) Western blot analysis of the relative expression of the indicated proteins in cells in (*B*). (*E*) Cell pellets of B16 melanoma cells stably expressing empty vector or Flag-UVRAG after four-day culture are shown. (*F*) Relative melanin contents in the cell lysates of (*E*), measured as optical density (OD) at 405 nm. Data are mean ± SD from three independent experiments. ****, $p < 0.0001$. (*G*)

Tyrosinase activity in extracts from cells in (*E*). n.s., not significant. (*H*) Quantitative RT-PCR showing the relative level of mRNA expression for TYR, TYRP1, and DCT in B16.Vector and B16.Flag-UVRAG cells in (*E*). Data are mean ± SD from three independent experiments. n.s., not significant. ****, $p < 0.0001$. (*I*) Western blot analysis of the relative expression of the indicated proteins in cells in (*E*). Actin serves as a loading control.

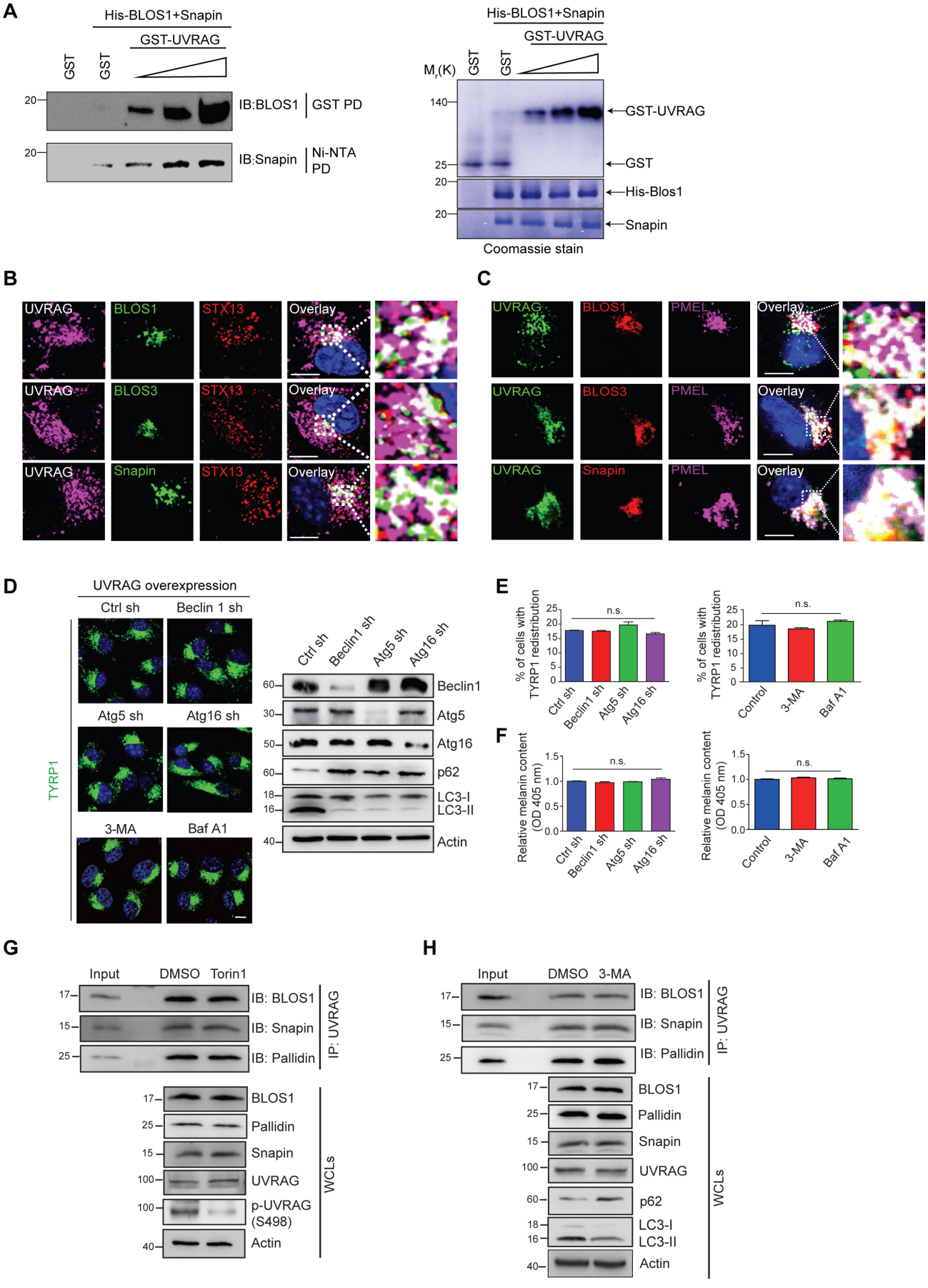
A
His-BLOS1+Snapin
GST-UVRAG
GST
GST
20
IB:BLOS1
GST PD
20
IB:Snapin
Ni-NTA PD
His-BLOS1+Snapin
GST-UVRAG
M_r(K)
GST
GST
140
GST-UVRAG
25
GST
20
His-Blos1
20
Snapin
Coomassie stain
B
UVRAG
BLOS1
STX13
Overlay
UVRAG
BLOS3
STX13
Overlay
UVRAG
Snapin
STX13
Overlay
C
UVRAG
BLOS1
PMEL
Overlay
UVRAG
BLOS3
PMEL
Overlay
UVRAG
Snapin
PMEL
Overlay
D
UVRAG overexpression
Ctrl sh
Beclin 1 sh
Atg5 sh
Atg16 sh
3-MA
Baf A1
TYRP1
Ctrl sh
Beclin1 sh
Atg5 sh
Atg16 sh
60
Beclin1
30
Atg5
50
Atg16
60
p62
18
16
LC3-I
LC3-II
40
Actin
E
% of cells with TYRP1 redistribution
n.s.
Ctrl sh
Beclin1 sh
Atg5 sh
Atg16 sh
% of cells with TYRP1 redistribution
n.s.
Control
3-MA
Baf A1
F
Relative melanin content (OD 405 nm)
n.s.
Ctrl sh
Beclin1 sh
Atg5 sh
Atg16 sh
Relative melanin content (OD 405 nm)
n.s.
Control
3-MA
Baf A1
G
Input
DMSO
Torin1
17
IB: BLOS1
15
IB: Snapin
25
IB: Pallidin
IP: UVRAG
17
BLOS1
25
Pallidin
15
Snapin
100
UVRAG
100
p-UVRAG (S498)
40
Actin
WCLs
H
Input
DMSO
3-MA
17
IB: BLOS1
15
IB: Snapin
25
IB: Pallidin
IP: UVRAG
17
BLOS1
25
Pallidin
15
Snapin
100
UVRAG
60
p62
18
16
LC3-I
LC3-II
40
Actin
WCLs

Fig. S2. Related to Fig. 2: UVRAG directly interacts with BLOS1 in melanosome biogenesis**.** (*A*) Purified recombinant UVRAG directly binds to recombinant BLOS1 and promotes the complex formation between BLOS1 and Snapin in vitro. Increasing amount of GST-UVRAG were mixed with purified His-BLOS1 and Snapin, and subjected to GST-pulldown (PD) or Ni-NTA PD, followed by IB for BLOS1 or for Snapin, as indicated. Coomassie blue stainings show input of each purified proteins used for binding. (*B*) Colocalization of UVRAG with the BLOC-1 complex proteins. B16 melanoma cells were immunostained with anti-UVRAG (purple), anti-STX13 (red), and anti-BLOS1 (green), anti-BLOS3 (green), or anti-Snapin (green), followed by confocal microscopy. Insets highlight UVRAG co-localization with BLOC-1 proteins. Scale bars, 20 μm. (*C*) Relative distribution of UVRAG and the BLOC-1 proteins with early stage of melanosomes. B16 melanoma cells were immunostained with anti-UVRAG (green), anti-PMEL (purple), along with anti-BLOS1 (red), anti-BLOS3 (red), or anti-Snapin (red), and followed by confocal microscopy. Scale bars, 20μm. (*D-F*) Autophagy is not required for UVRAG-mediated melanosome pigmentation. B16 melanoma cell stably expressing UVRAG was transfected with control shRNA or shRNA against Beclin1, Atg5, or Atg16, or treated with 3-MA (1 mM, 48 hrs) or Bafilomycin A1 (Baf A1 10 nM, 12 hrs), and then stained for TYRP1 (green) (*D*). Nuclei were stained with DAPI (blue). Endogenous protein expression and the autophagy levels (p62 and LC3-II levels) in the indicated cells is also shown by immunoblotting (right). The redistribution of TYRP1 (*E*) and the relative melanin contents in the cell lysates of (*F*) in cells in (*D*) was quantified. n.s., not significant. Scale bar, 10 μm. (*G,H*) Interaction between UVRAG and BLOS1 is not affected by the mTOR inhibitor Torin1 (*G*) and by the Vps34 inhibitor 3-MA (*H*). WCLs of B16 cells treated with Torin1 (1 μM, 1 hr) or 3-MA (1 mM, 48 hrs) were immunoprecipitated with anti-UVRAG antibody followed by immunoblotting with the antibodies as indicated. Note that Torin1 treatment suppressed mTORC1-mediated S498 phosphorylation of UVRAG; and that 3-MA inhibited autophagy as indicated by increased levels of p62 and reduced production of LC3-II. Actin serves as a loading control.

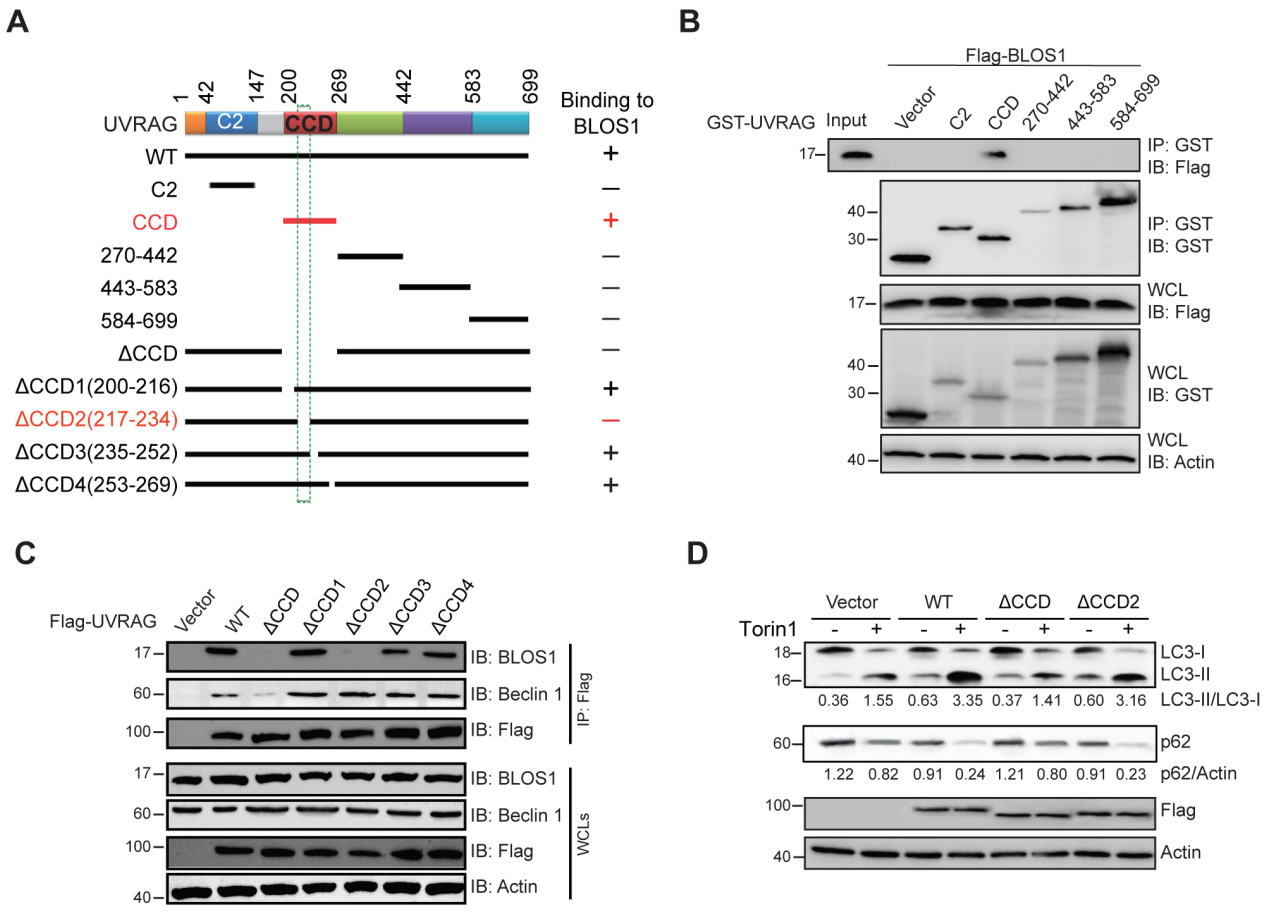

Fig. S3. Related to Fig. 2: Domain mapping of UVRAG interactions with BLOS1. (*A*) Schematic representation of WT UVRAG and its deletion mutants and summary of their interactions with BLOS1. (*B*) UVRAG CCD interacts with BLOS1. 293T cells were co-transfected with Flag-BLOS1, together with GST-tagged vector or UVRAG mutants as indicated. At 48 hr post-transfection, WCL were used for GST-pull down, followed by IB with indicated antibodies. (*C*) Deletion of CCD2 (residues 217-234) in UVRAG abolished UVRAG interaction with endogenous BLOS1 but had no effect on UVRAG interaction with endogenous Beclin1. (*D*) Western blot analysis and densitometric quantification (underneath the blots) of the LC3-II/LC3-I ratios and the p62/actin in the indicated cells treated with Torin1. Note that ΔCCD2 mutant, albeit defective in BLOS-1 binding, remains competent in Torin1-induced autophagy activation. Data are representative of three independent experiments.

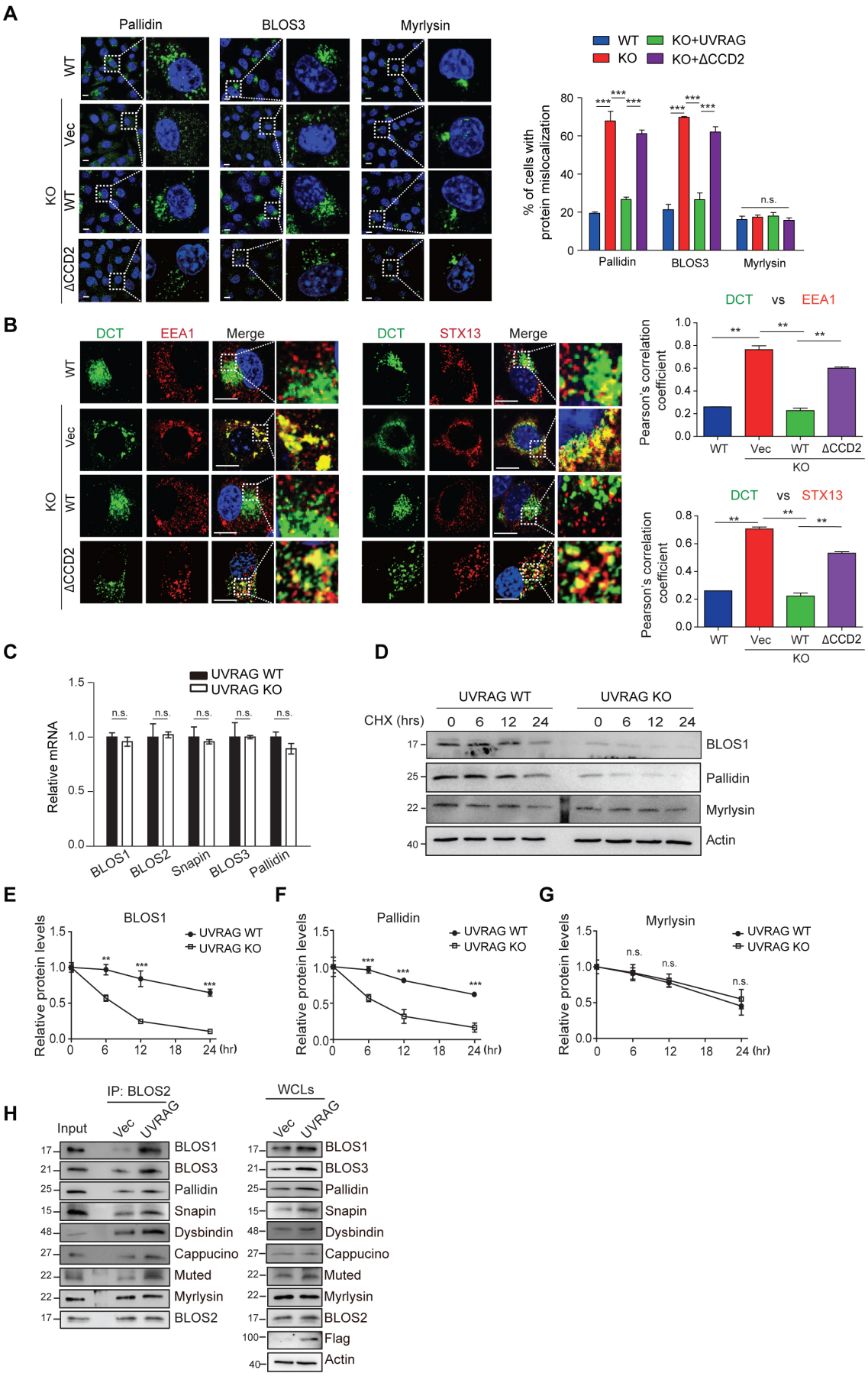
A
Pallidin
BLOS3
Myrlysin
WT
KO
Vec
WT
ΔCCD2
WT
KO+UVRAG
KO
KO+ΔCCD2
% of cells with protein mislocalization
Pallidin
BLOS3
Myrlysin
n.s.
B
DCT
EEA1
Merge
DCT
STX13
Merge
DCT vs EEA1
DCT vs STX13
Pearson's correlation coefficient
WT
Vec
WT
ΔCCD2
KO
C
UVRAG WT
UVRAG KO
Relative mRNA
n.s.
BLOS1
BLOS2
Snapin
BLOS3
Pallidin
D
UVRAG WT
UVRAG KO
CHX (hrs)
0 6 12 24 0 6 12 24
BLOS1
Pallidin
Myrlysin
Actin
E
BLOS1
F
Pallidin
G
Myrlysin
UVRAG WT
UVRAG KO
Relative protein levels
(hr)
H
IP: BLOS2
WCLs
Input
Vec
UVRAG
BLOS1
BLOS3
Pallidin
Snapin
Dysbindin
Cappucino
Muted
Myrlysin
BLOS2
Flag
Actin

Fig. S4. Related to Fig. 2: UVRAG is required for the proper distribution, cargo sorting function, and protein stability of BLOC-1. (*A*) Cytoplasmic distribution of Pallidin, BLOS3, or Myrlysin in *UVRAG* WT and KO cells and KO cells with the complementation of WT UVRAG or UVRAG ΔCCD2 mutant. The percentage of cells with the aberrant distribution of the indicated protein was quantified (right panel). Means were calculated from the data collected from three independent experiments (n = 200). ***, $p < 0.001$. n.s., not significant. Scale bars, 10 μm. (*B*) The melanosomal cargo protein DCT is mislocalized to EEA1- and STX13-positive endosomes in *UVRAG* WT and KO cells and KO cells with the complementation of WT UVRAG or UVRAG ΔCCD2 mutant. Cells as indicated were immunostained with anti-DCT (green), anti-EEA1 (red) or anti-STX13 (red), followed by confocal microscopy. The degree of colocalization between endogenous DCT with EEA1 or STX13 in the cells is shown (right). Means were calculated from the data collected from three independent experiments (n = 50). **, $p < 0.01$. Scale bars, 20 μm. (*C*) Knockout of UVRAG has no effect on mRNA levels of BLOC-1 proteins. n.s., not significant. (*D-G*) Immunoblot of *UVRAG* KO melanocytes treated with CHX for the indicated time points shows a decrease in steady-state levels and stability of BLOS1 and Pallidin, but not Myrlysin, upon loss of UVRAG, as indicated by the densitometric quantification (*E-G*) of the relative expression of the indicated proteins in cells in (*D*). Data are representative of three independent experiments. **, $p < 0.01$; ***, $p < 0.001$; n.s., not significant. (*H*) UVRAG overexpression increased the complex assembly of BLOC-1. WCLs of B16 cells stably expressing vector control or Flag-UVRAG were immunoprecipitated with anti-BLOS2 antibody, followed by immunoblotting analysis with the indicated antibodies. Actin serves as a loading control. Data are representative of three independent experiments.

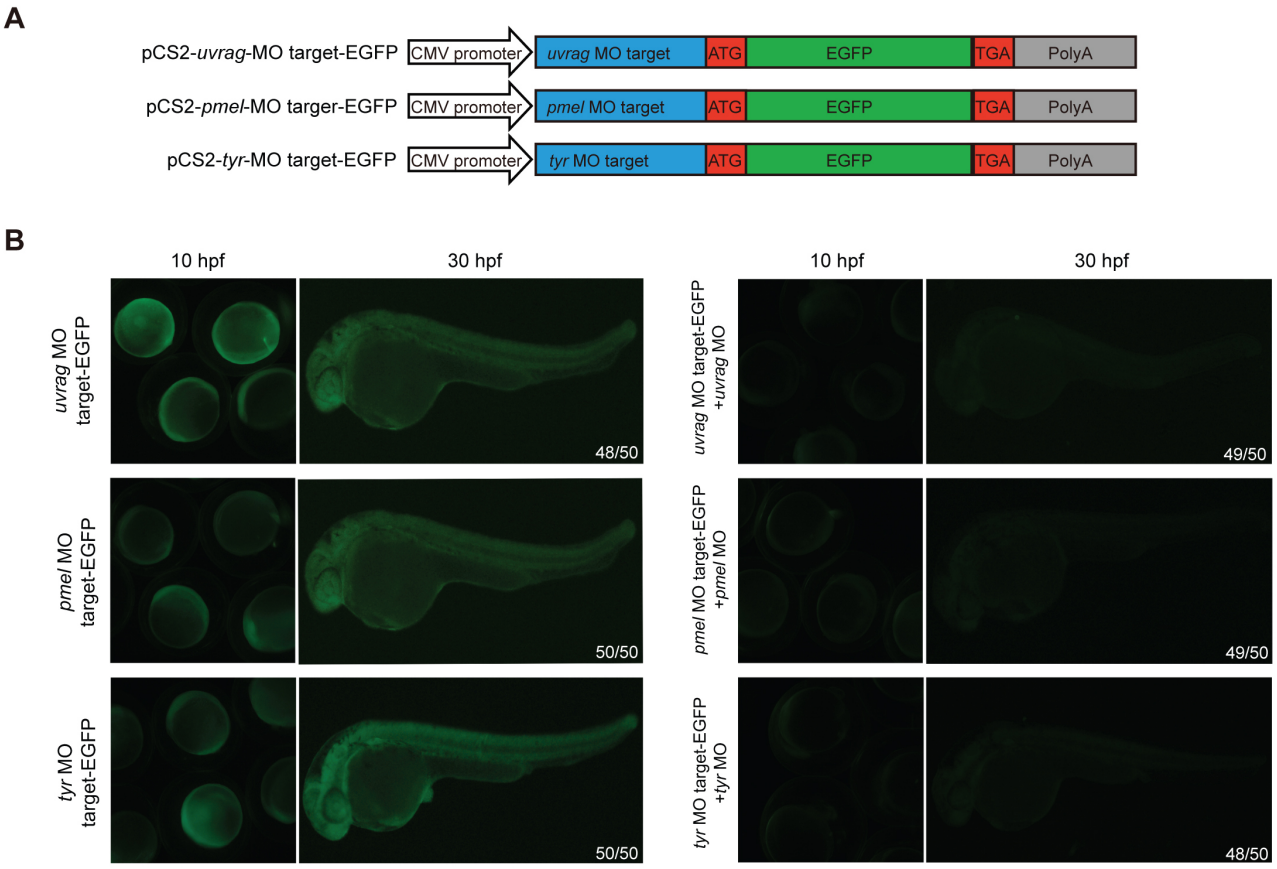

Fig. S5. Related to Fig. 3: Effect of UVRAG deficiency on melanosome biogenesis *in vivo*. (*A*) Schematic representation of injected vectors containing the morpholino (MO) target sequence fused to GFP. The target site of *uvrag, tyr, and pmel* is fused to the 5' of GFP. (*B*) Efficacy and specificity of *uvrag, pmel,, and tyrosinase (tyr)* MO. Left panels show Zebrafish embryos injected with the MO target-GFP fusion constructs as indicated. Right panels show co-injection of both MO target-GFP fusion constructs and MOs as indicated. Embryos were imaged at 10 hrs and 30 hrs post-fertilization (hpf) with the exposure time of 1.5 s in all groups. The disappearance of GFP expression (right panels) highlights the specific depletion of the target gene in Zebrafish embryos.

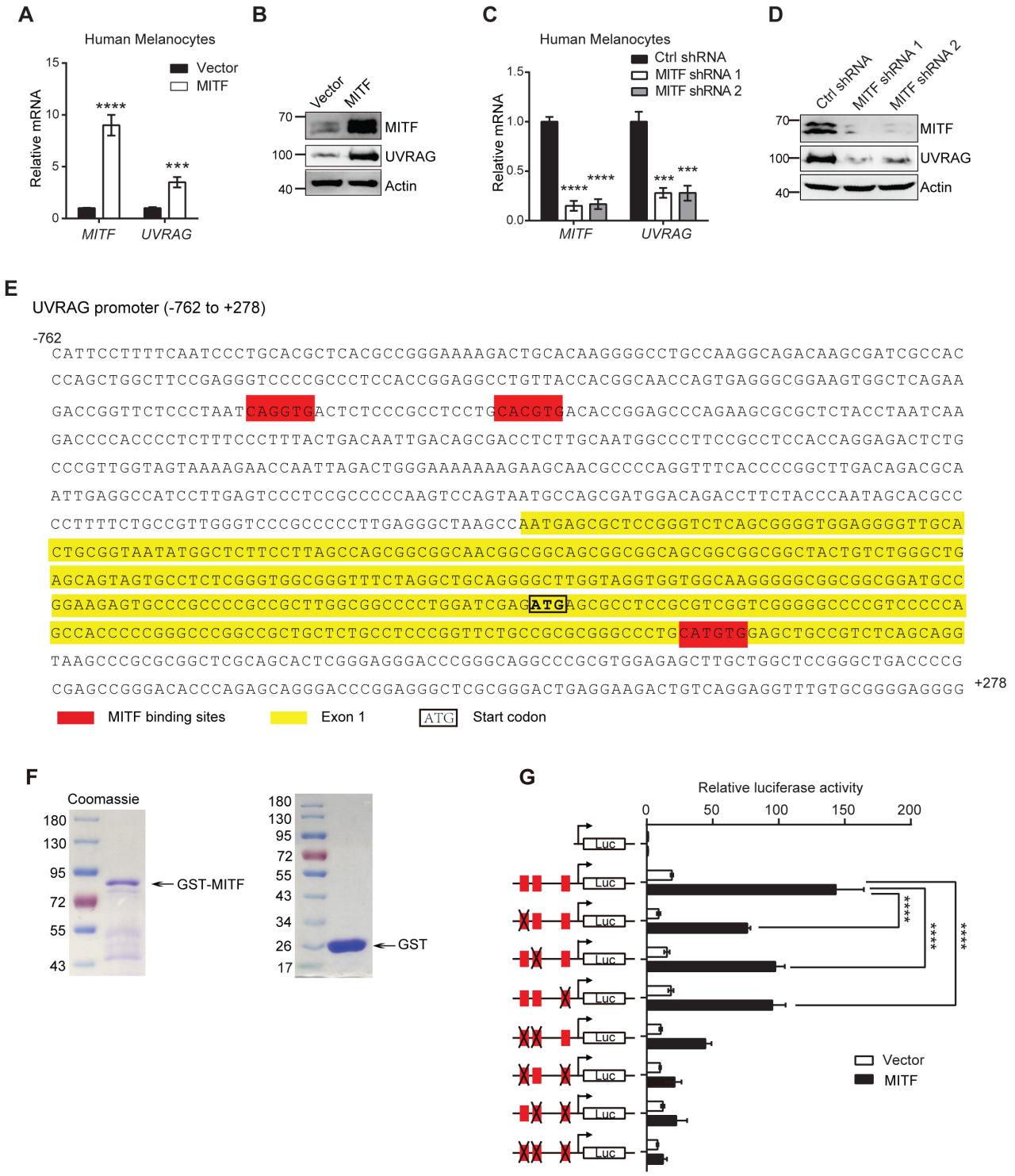

Fig. S6. Related to Fig. 4. *UVRAG* is a direct transcriptional target of MITF. (*A*) *UVRAG* mRNA expression in human primary melanocytes stably expressing Flag-MITF *versus* Vector control. Data are mean ± SD from three independent experiments. ***, $p < 0.001$; ****, $p < 0.0001$. (*B*) Western blot analysis of the relative expression of *UVRAG* in the indicated cells, as in (*A*). (*C*) *UVRAG* mRNA expression in human melanocytes expressing control shRNA or two independent shRNA against MITF. Data are mean ± SD from three independent experiments. ***, $p < 0.001$; ****, $p < 0.0001$. (*D*) Western blot analysis of the relative expression of UVRAG in the indicated cells, as in (*C*). (*E*)

Schematic view of human *UVRAG* promoter showing the sequence of the MITF (red)-binding sites. (*F*) Coomassie-staining of purified recombinant GST-MITF (left) and GST control (right) proteins. (*G*) Dual luciferase reporter assay showing the activity of *UVRAG* promoters harboring different E box mutations as indicated in 293T cells transfected with MITF. Note that mutations in either E box suppress activity of *UVRAG* promoter. Error bars represent SD mean of at least three independent experiments. ****, $p < 0.0001$.

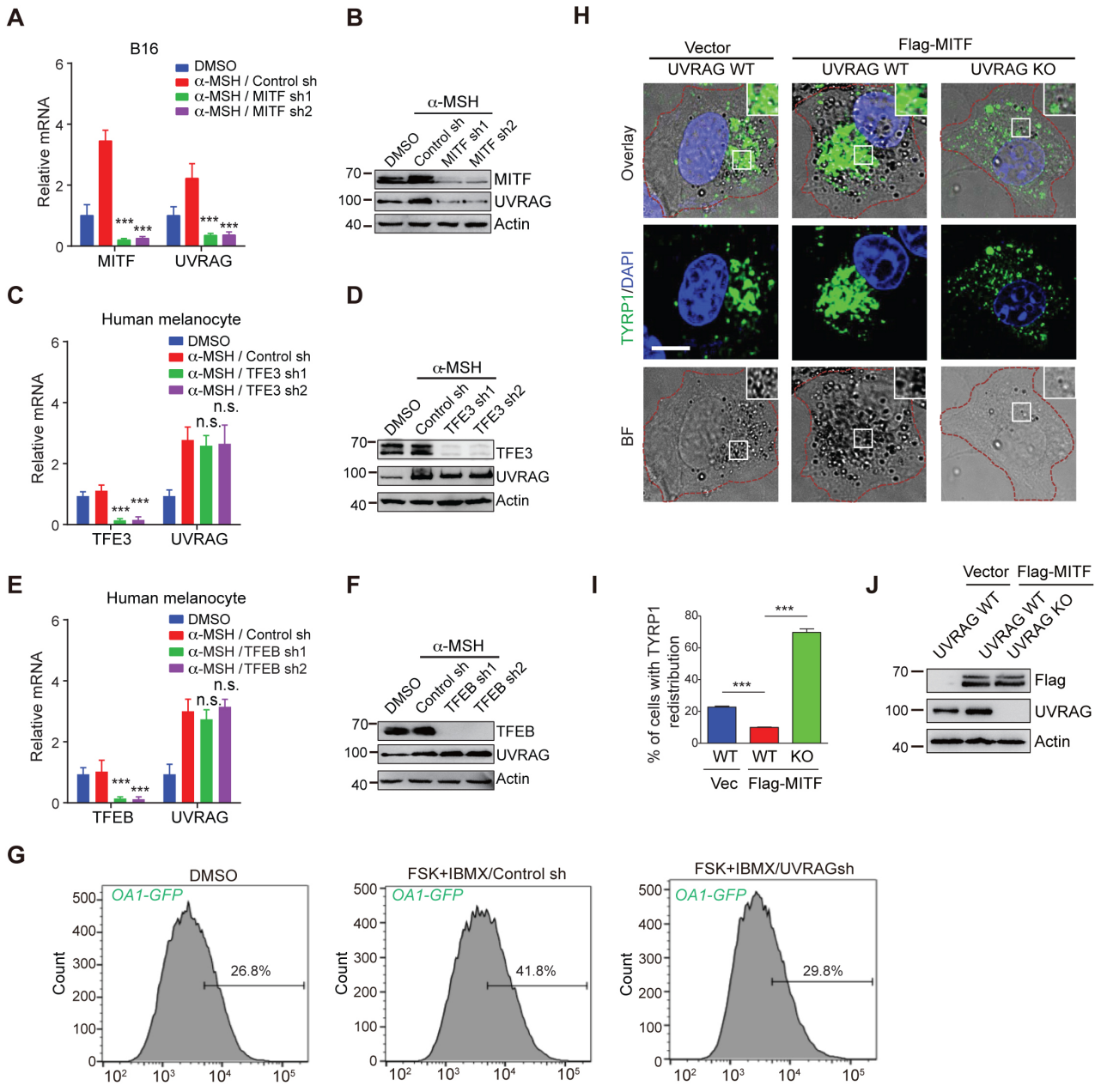

Fig. S7. Related to Fig. 5: Response of UVRAG to α-MSH signaling. (*A*) *UVRAG* mRNA expression in B16 melanoma cells expressing two independent shRNA against MITF and treated with α-MSH for 2 hr. Data are mean ± SD from three independent experiments. ***, $p < 0.001$. (*B*) Western blot analysis of the relative expression of MITF and UVRAG in cells in (A) in response to α-MSH treatment. (*C*) *UVRAG* mRNA expression in human melanocytes expressing two independent shRNA against TFE3 and treated with α-MSH for 2 hr. Data are mean ± SD from three independent experiments. n.s., not significant; ***, $p < 0.001$. (*D*) Western blot analysis of the relative expression of TFE3 and UVRAG in cells in (*C*) in response to α-MSH treatment. (*E*) *UVRAG* mRNA expression in human melanocytes expressing two independent shRNA against TFEB and treated with α-MSH for 2 hr. Data are mean ± SD from three independent experiments. n.s., not significant; ***, $p < 0.001$. (*F*) Western blot analysis of the relative expression of MITF and UVRAG in cells in (*E*) in response to α-MSH treatment. (*G*) Depletion of UVRAG suppresses cAMP agonists-induced melanogenesis. B16 cells stably expressing

melanosome marker OA1-GFP were transfected with control shRNA or UVRAG-specific shRNA and treated with forskolin (Fsk)+IBMX for 2 hrs. The resultant cells were subjected to flow cytometry analysis. The portion of cells with the fluorescence intensity greater than the indicated threshold is indicated. Data are representative of three independent experiments. (*H-J*) Bright-field (BF) and confocal microscopy analyses of cell pigmentation and the distribution of TYRP1 in *UVRAG* WT and KO B16 cells expressing either empty vector or Flag-MITF (*H*). The percentage of cells with the redistribution of TYRP1 was quantified in (*I*). Data are mean ± SD from three independent experiments. Flag-MITF and endogenous UVRAG expression were confirmed by immunoblotting (*J*). ***, $p < 0.001$. Scale bar, 20 μm.

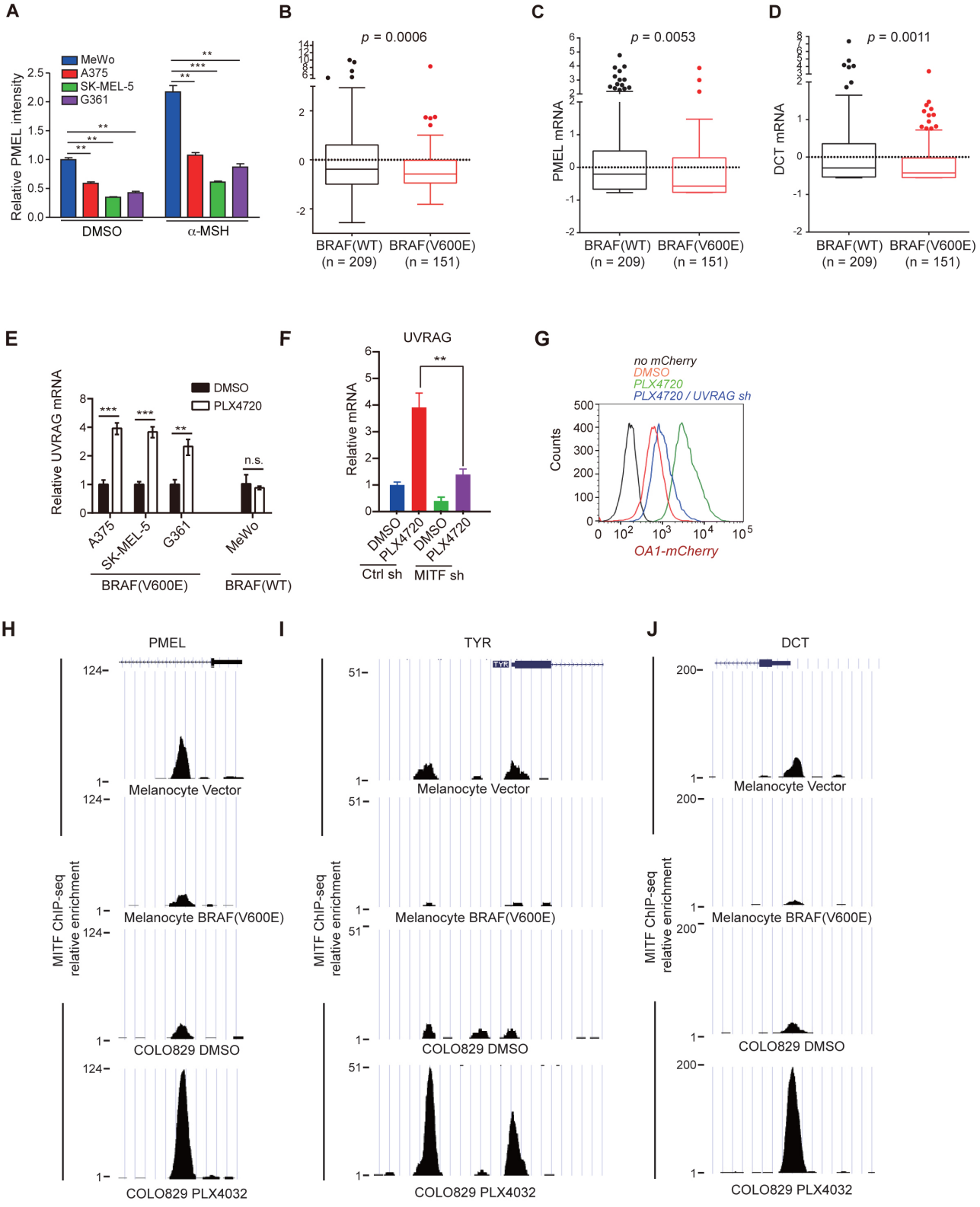

Fig. S8. Related to Fig. 6: Oncogenic BRAF inhibits MITF-regulated melanogenic gene expression and melanogenesis. (*A*) BRAF(V600E)-positive human melanoma cells show reduced response to α-MSH-induced melanogenesis than BRAF(WT) melanoma cells. Human melanoma cells as indicated

were treated with DMSO or α-MSH for 2 hrs. The relative intensity of PMEL in these cells was quantified by confocal microscopy analysis. Data are mean ± SD (n = 150 cells from three independent experiments). **, $p < 0.01$; ***, $p < 0.001$. (*B-D*) Box plots showing expression levels (Z-score) of *UVRAG* (*B*), *PMEL* (*C*), and *DCT* (*D*) in melanoma patients with BRAF WT or V600E mutant from the TCGA database. Note that BRAF(V600E) is negatively associated with the gene expressions. *p*, unpaired *t* test. (*E*) Quantitative RT-PCR showing the relative mRNA expression for *UVRAG* in human melanoma cells that are BRAF WT or BRAF V600E, treated with PLX4720 (1 μM) for 48 hrs. Data are mean ± SD from three independent experiments. n.s., not significant; **, $p < 0.01$; ***, $p < 0.001$. (*F*) Quantitative RT-PCR showing the relative mRNA expression for *UVRAG* in A375 cells expressing control shRNA or *MITF*-specific shRNA and treated with PLX4720 (1 μM). Data are mean ± SD from three independent experiments. **, $p < 0.01$. (*G*) A375 melanoma cells expressing control shRNA or *UVRAG*-specific shRNA were treated with PLX4720 (1 μM) and subjected to flow cytometry analysis using OA1-mCherry as a marker of melanosomes. Data are representative of three independent experiments. (*H-J*) ChIP-seq analysis of the occupancy of MITF on the promoter of *PMEL* (*H*), *TYR* (*I*), and *DCT* (*J*) in melanocytes transduced with either empty vector (1st row) or BRAF(V600E) (2nd row); as well as in BRAF(V600E)-positive COLO829 melanoma cells treated with DMSO (3rd row) or with PLX4032 (4th row) . The original data of ChIP-seq is obtained from the previous study(10).

Table S1. Identification of UVRAG-interacting proteins

Gene	Description	Number of clones isolated
BECN1	Beclin 1	4
CEP63	Centrosomal protein 63	9
DCTN2	Dynactin subunit 2	3
TRIP11	Thyroid Hormone Receptor Interactor 11	3
SNX1	Sorting nexin 1	2
Furin	Paired basic amino acid cleaving enzyme	1
BLOS1	Biogenesis of lysosomal organelles complex 1 subunit 1	5
Snapin	SNAP associated protein	1
TMEM9	Transmembrane protein 9	2
TSG101	Tumor susceptibility 101	1
Vps27	Vacuolar protein sorting-associated protein 27	1
CLU	Clusterin	1

Table S2: List of Primers Used in the Study.

I: Primers used for quantitative PCR.

Gene	Species	Forward (5'-3')	Reverse (5'-3')
Actin	H	GCTCGTCGTCGACAACGGCT	CAAACATGATCTGGCTCATCTTCTC
TYR	H	GTCCACTTACTGGGATAGCG	AGTCTGGGTCTGAATCTTGTAG
TYRP1	H	AAGTATGACCCTGCTGTTCG	CATAAGTGTATCCCAGGTTGTC
DCT	H	GTTTGATAAAGCAGATGGGACT	ACTGGAGGGAAGAAAGGAA
UVRAG	H	AGGATTACTTTGTATGCGGTGTC	CAGGTTGGGAAGGGTTTGC
MITF-M	H	TCCTGTCCAGCCAACCTTCC	TGATGATCCGATTCACCAAAT
PMEL	H	AGGGTATTGAAAGTGCCGAGAT	CAGCCATCAACACCAGCAAG
TFE3	H	ACCAGCTCGGGATGGCGTAG	CAGCAAGACCCTCGATGAAGAAG
TFEB	H	GGCAACAGTGCTCCCAATAGC	CCCAACTCCTTGATGCGGTCA
MITF-M	M	AGCAAGAGCATTGGCTAAAGA	GTGGATGGGATAAGGGAAAGT
TFE3	M	CTGAAGGCATCTGTGGATTACATC	CAAGTGGTCGCTGGGAAAGT
PMEL	M	CCTCTACTGGATGACACCGACAC	TGAGCCACCTTTCAGCACTT
UVRAG	M	AAGGATTATTTTGTATGTGGTGTC	CAGGTTAGGAAGAGTTTGC
TYR	M	GTCCACTCACAGGGATAGCA	AGCCTGGATCTGACTCTTGGAG
Actin	M	GCTGGTCGTCGACAACGGCT	CAAACATGATCTGGGTCATCTTTTC
TYRP1	M	AAATATGACCCTGCTGTTCG	CATAAGCATATCCCAGATTGTC
DCT	M	GTTTGATAAAGCAGACGGAACA	ACCGGTGGGAAGAAGGGGA
BLOS1	M	CCCAGGCCTACATGAACCAG	CCATTCCAATCCACTGGCCT
BLOS2	M	TGACAGCCACCAGTGAAGAC	TCCTTCAGGTTTCTGCTGATGT
BLOS3	M	TGGATATCGTGGCTGGCTGT	GTCCTGCTCGGGCTCCATAC
Snapin	M	GCTACAGAACTGTGCCGGAT	AACCGCCTTAGTCGTTCCTG
Pallidin	M	AGATCTGCAGAGGTCCAAGC	TGTCCAACATGGAGTGGCAT
H, human; M, mouse			

II. Primers used for generating *UVRAG* knockout cell by CRISPR-Cas9 nickase

Primer Name	Forward (5'-3')	Reverse (5'-3')
UVRAG sgRNA 1	CCGGGTGGACCCCTGAGCCGCCGAG	AAACCTCGGCGGCTCAGGGGTCCAC
UVRAG sgRNA 2	CCGGGGAGCTCCTGCGCCTCGCTCG	AAACCGAGCGAGGCGCAGGAGCTCC

III. Primers used for the mutagenesis of gene promoters

Target	Forward (5'-3')	Reverse (5'-3')
***UVRAG* promoter**	TAATAGAATAATCCAGACCCACG	CCCTCCCCGCACAAACCTCCT
E box1-mutated *UVRAG* promoter	ACTCTCCCGCCTCCTG	ATTAGGGAGAACCGGTCT
E box2-mutated *UVRAG* promoter	ACACCGGAGCCCAGAA	CAGGAGGCGGGAGAGT
E box3-mutated *UVRAG* promoter	GAGCTGCCGTCTCAGCA	CAGGGCCCGCGCGGCAG
DCT promoter	CTGAATAGGAGAAGAGTAAGTTA	ACTAGAGGGTGTGAAGAATAAAC
TYR promoter	TGAGATATCCCCACAATGAAGCA	TTGTCCTTCTCTGGGGCACTCAA
BS: binding site		

IV. Primers for ChIP analysis

Gene	Forward (5'-3')	Reverse (5'-3')
***IRF4* Intron 4 for TFAP2A binding**	CTTCAGGCTTTCTTGATGTGAA	GGAGGATCATAAAGGACAATGG
***TYR* Pro for YY1**	TTGTACTGCCTGCTGTGGAG	CAGGAACCTCTGCCTGAAAG
***TYR* Pro for MITF**	ACGAGCCAATTCGAAAGAAA	CACAGATTTCTCTTTCCAGCTAC
UVRAG Pro for MITF	TTACCACGGCAACCAGTGAGG	AATTGTCAGTAAAGGGAAAGAGGG
UVRAG Pro for YY1	AGGAGACTCTGCCCGTTGGT	GGCGTGCTATTGGGTAGAAGGT
UVRAG Pro for TFAP2A	CTCAGCGGGGTGGAGGGGTTG	ACGCGGAGGCGCTCATCTCG
GAPDH	GGCAGCACAGCCCACAGGTT	ATCGTGACCTTCCGTGCAGAAAC

V. Probes for EMSA assay

EMSA Probe	Forward (5'-3')	Reverse (5'-3')
UVRAG E box1&2	CAGCTGGCTTCCGAGGGT	AGAGGTCGCTGTCAATTG
UVRAG E box 3	ATGAGCGCCTCCGCGTCGGTC	CCCTCCCCGCACAAACCTCCT
UVRAG E box 1 mutated	ACTCTCCCGCCTCCTG	ATTAGGGAGAACCGGTCT
UVRAG E box 2 mutated	ACACCGGAGCCCAGAA	CAGGAGGCGGGAGAGT
UVRAG E box 3 mutated	GAGCTGCCGTCTCAGCA	CAGGGCCCGCGCGGCAG

References

1. Liang C*, et al.* (2008) Beclin1-binding UVRAG targets the class C Vps complex to coordinate autophagosome maturation and endocytic trafficking. *Nat Cell Biol* 10(7):776-787.
2. Jebreel A*, et al.* (2007) Investigation of interleukin 10, 12 and 18 levels in patients with head and neck cancer. *The Journal of laryngology and otology* 121(3):246-252.
3. Rad HH*, et al.* (2004) Tyrosinase-related proteins suppress tyrosinase-mediated cell death of melanocytes and melanoma cells. *Exp Cell Res* 298(2):317-328.
4. Yao C, Jin CL, Oh IG, Park CH, & Chung JH (2015) Melia azedarach extract stimulates melanogenesis through increase of tyrosinase-related protein 1 expression in B16F10 mouse melanoma cells. *Int J Mol Med* 35(6):1761-1766.
5. Lee JS*, et al.* (2009) FLIP-mediated autophagy regulation in cell death control. *Nat Cell Biol* 11(11):1355-1362.
6. Rathmell WK & Chu G (1994) A DNA end-binding factor involved in double-strand break repair and V(D)J recombination. *Mol Cell Biol* 14(7):4741-4748.
7. Rodrigue A*, et al.* (2006) Interplay between human DNA repair proteins at a unique double-strand break in vivo. *Embo J* 25(1):222-231.
8. Berson PJ (2001) The porcelain-fused-to-metal telescope: a simple approach to salvaging existing crowns with recurrent decay. *Gen Dent* 49(5):470-472.
9. Debec A*, et al.* (2001) Toucan protein is essential for the assembly of syncytial mitotic spindles in Drosophila melanogaster. *Genesis* 31(4):167-175.
10. Webster DE*, et al.* (2014) Enhancer-targeted genome editing selectively blocks innate resistance to oncokinase inhibition. *Genome Res* 24(5):751-760.
11. Li J*, et al.* (2012) YY1 regulates melanocyte development and function by cooperating with MITF. *PLoS Genet* 8(5):e1002688.
12. Cerami E*, et al.* (2012) The cBio cancer genomics portal: an open platform for exploring multidimensional cancer genomics data. *Cancer discovery* 2(5):401-404.
13. Gao J*, et al.* (2013) Integrative analysis of complex cancer genomics and clinical profiles using the cBioPortal. *Science signaling* 6(269):pl1.